Utilization of Oil Palm Trunk Waste for Manufacturing of Binderless Particleboard: Optimization Study

Wan Noor Aidawati Wan Nadhari,[a] Rokiah Hashim,[a,*] Othman Sulaiman,[a] Masatoshi Sato,[b] Tomoko Sugimoto,[c] and Mohd Ezwan Selamat [a]

Utilization of oil palm trunk waste for production of environmental friendly binderless particleboard was studied. Response surface methodology was used to optimize the manufacturing conditions. The steaming temperature (100 to 120˚C), steaming time (25 to 50 min), hot pressing temperature (180 to 220˚C), and hot pressing time (15 to 30 min) were optimized in the ranges shown. The optimum conditions for making the particleboard were found to involve steaming for 46 min at a temperature of 120˚C before it was compressed using a pressure of 12 MPa, at a temperature 215 ˚C for 29 min. The internal bond (IB) strength, modulus of rupture (MOR), thickness swelling (TS), and water absorption (WA) were 0.54 MPa, 8.18 MPa, 22%, and 51%, respectively. The residual values of actual and model-based calculated IB, MOR, TS, and WA were found to be 0.1 MPa, 0.23 MPa, 2%, and 4%, respectively, which shows the significance of the study.

Keywords: Oil palm trunk waste; Particleboard; Binderless; Steaming; Optimization.

*Contact information: a: Division of Bio-resource, Paper and Coatings Technology, School of Industrial Technology, Universiti Sains Malaysia, 11800 Minden, Penang, Malaysia; b: Graduate School of Agricultural and Life Sciences, The University of Tokyo, 1-1-1, Yayoi, Bunkyo-ku, Tokyo 113-8657, Japan; C: Japan International Research Center for Agricultural Sciences, 1-1, Owashi, Tsukuba, Ibaraki 305-8686, Japan; * Corresponding author: Email address: hrokiah@usm.my (R.Hashim) Tel.: +60 4 6535217; fax: +60 4 6573678*

INTRODUCTION

Particleboard is an engineered material that can be classified as a composite panel. It has been widely utilized in many industrial and domestic applications for structural components in furniture or architecture, and it is in high demand as a building material. Its performance is dependent on the properties of the wood species, resin, manufacturing approach, and production process. According to current practices, commercial particleboard causes the emission of volatile organic compounds from the resins; since these are mostly formaldehyde-based adhesives, this may result in environ-mental and health concerns due to the formaldehyde released. The worldwide trend signifies that the marketplace is moving towards using particleboard with a small amount or no formaldehyde (Hashim *et al*. 2009). Resin-containing panels are not only expensive but are also made from nonrenewable resources.

Binderless particleboard is a panel formed without using any synthetic resins. It can be prepared by hot pressing, involving a so-called self-bonding process, wherein the adhesion is derived from activating chemical components of the board constituents (Sasaki 1980). Such an approach is less hazardous, and the products are biodegradable and environmentally friendly, particularly in terms of waste disposal and recycling. Moreover, resins are expensive and contribute to a relatively high cost in particleboard manufacturing.

Abolishing or reducing the use of resin has potential to reduce the cost of particleboard manufacture such that the product can be made available at a cheaper price (Pandey and Nema 2004). Binderless board can be used as an interior building material, green packaging product, and also as a decorative material.

Nowadays, scarcity of wood as a raw material in wood-based industries has motivated producers to find a substitute for wood. The expansion of oil palm plantations has resulted in significant amounts of residue at harvesting sites (Hashim *et al.* 2010). Great quantities of oil palm trunks are left in cultivated areas without being fully utilized and are regarded as wastes. Oil palm trunk is a lignocellulosic material consisting of parenchyma and vascular bundles. It can work as a green material to meet future industry needs because of its availability and sustainability. Oil palm trunk has a high starch content (12.19-17.17%) and sugar content; glucose (5.97-6.55%), xylose (6.20-6.55%), and arabinose (1.09-1.31%) that could probably help the self-bonding in binderless particleboard (Hashim *et al.* 2011).

Previous studies have indicated that steam pressure and treatment time affect the properties of binderless particleboard. The bending and internal bond strength have been improved with steam treatment. A long steam treatment time was shown to contribute low thickness swelling (TS) values and thus better dimensional stability (Xu *et al.* 2003). Steam treatment tends to hydrolyze the hemicellulose and lignin to make them softer. Boards made from oil palm frond fibers treated under a steam pressure exhibited the highest strength (Laemsak and Okuma 2000). A decrease in hemicellulose has been shown to be directly related to the increase in the dimensional stability of the boards (Velásquez *et al.* 2003). It was also suggested that lignin and furfural derivatives were produced during steam explosion, and their presence contributed to self-bonding of the steam exploded oil palm fronds pulps (Suzuki *et al.* 1998).

The objective of this study was to establish the optimum conditions for making environmentally and sustainable binderless particleboard from oil palm trunk waste by using response surface methodology (RSM). A rotatable central composite design (RCCD) was selected to optimize the manufacturing variables of the board making. The effects of manufacturing variables such as steaming temperature, steaming time, hot pressing temperature, and hot pressing time were evaluated relative to the mechanical and dimensional stability properties of binderless particleboard using oil palm trunk waste. The RSM has many advantages such as a significant reduction in the number of costly experiments, knowledge of effective parameters, the possibility to evaluate the effect of interactions between the parameters, better precision of results, and mathematical modeling of experiments (Ahmadi *et al.* 2005; Chang *et al.* 2006). Although the RSM is largely employed in the optimization of industrial processes, it has not been applied so far to determine the conditions of binderless particleboard, especially using pre-treated waste raw materials.

EXPERIMENTAL

Sample Preparation and Board Making Procedure

Oil palm trunks with an approximate age of 25 years old were harvested from a local plantation in Northern Malaysia. After being felled, the trunks were immediately cut into discs, chopped into chips, and steamed at a temperature range of 100 to 120˚C for a period of 25 to 50 min by using autoclave model Hirayama (HVE-50). They were dried

and ground to a particle size in the range of 15 to 2000 µm using the particle size analyzer model Mastersizer 2000 version 5.60. The 65% average size were from the range of particles size between 316 and 1445 µm were air-dried until the moisture content reached a constant value of around 7 to 8%. Single-layer particleboards without using any adhesives were manufactured at a density of 0.8 g/cm^3 in the laboratory after the particles were hand-formed in the 20.5 x 20.5 cm mould. The particleboards were hot pressed at temperature (180 to 220˚C) for (15 to 30 min) and 12 MPa pressure, by using the distance bar of 0.5 cm as the board thickness. These manufacturing conditions range were selected based on the preliminary study.

The boards were kept in a conditioned room to equilibrate them at 20 ±2˚C and 65 ±2% relative humidity (RH) until the moisture content of particleboards was constant at around 8%. The boards were cut into specimens for mechanical and physical testing in terms of internal bond (IB) strength, bending strength (MOR), thickness swelling (TS), and water absorption (WA).

Mechanical and Physical Testing Methods of Board

For internal bond (IB) strength and bending strength, the test samples were evaluated according to the Japanese Industrial Standards (JIS A 5908-2003) using an INSTRON Gotech Testing Machine (GT-AL-7000L). The IB strength was calculated using the board specimen of dimension 5 cm x 5 cm x 0.5 cm. A tensile force was applied at a loading speed of 2 mm/min (JIS A 5908-2003) for IB strength and 10 mm/min for bending strength. The IB strength for each sample was calculated using following Eq. (1),

$$IB = \frac{P}{b \times L} \quad (1)$$

where P is the maximum load at the time of failing force in units N, b is the width of test specimen in units of mm, and L is the length of sample in units of mm.

The bending strength in terms of modulus of rupture (MOR) of individual test specimen was calculated using following Eq. (2),

$$MOR = \frac{3 \times P \times dL}{2 \times b \times t^2} \quad (2)$$

where P is the maximum load in units of N, dL is the span length in units of mm, b is the width of test specimen in units of mm, and t is the thickness of test specimen in units of mm.

For the thickness swelling (TS) test, the thickness (in *mm*) of the test specimen before immersion in water was taken as t_1. The specimen was immersed horizontally about 3 cm deep in water maintained at temperature 20±1 °C for 24 h, then the thickness was measured as t_2. The swelling in thickness after immersion in water was calculated using Eq. (3):

$$TS(\%) = \frac{(t_2 - t_1) \times 100}{t_1} \quad (3)$$

The water absorption (WA) test analyzed the dimensional stability of the panel (Mancera *et al.* 2012). The initial weight of the test specimen was taken as W_1. After immersion in water (maintained at temperature 20±1 °C) for 24 h, the test specimen were reweighed and taken as W_2. Water absorption of test specimen was calculated using Eq. (4):

$$WA(\%) = \frac{(W_2 - W_1) \times 100}{W_1} \quad (4)$$

Response Surface Methodology Approach

Response surface methodology (RSM) is a commonly practiced statistical tool for the optimization of manufacturing processes. It optimizes the operating factors to give a desired response within a limited number of experiments. The operating factors selected for optimization were steaming temperature, steaming time, hot pressing temperature, and hot pressing time. The desired responses were observed in terms of internal bond strength, modulus of rupture, thickness swelling, and water absorption to produce quality binderless particleboard. The rotatable central composite design was used to select the different combinations of operating factors. With this design one can extrapolate and interpolate the obtained data in a manner that gives the freedom to observe the effect of the operating factors beyond its data points. The RCCD design is effective in fitting the experimental data into a linear, second order, or cubic mathematical models and is useful in analyzing the interaction between the operating factors.

For four operating factors the rotatable central composite design consists of 2^4 factorials runs (coded to the usual (±1, ±1, ±1, ±1) notation) with 2x4 axial runs (coded in (±2,0,0,0), (0, ±2,0,0), (0,0, ±2,0) and (0,0,0, ±2) notation) and 6 replicates at the central runs (coded in (0,0,0,0) notation). The reproducibility and experimental error of the data were evaluated by the center points runs. The benefit of the rotatable design is to allow the variance of the model prediction to a constant value and fixed the operating factors data set of the model equidistant from the center point of the design and each variable can be investigated at two levels. Analysis of variance (ANOVA) was used to analyze the model, responses, and its corresponding operating factors.

The optimized binderless particleboard characterized by internal bond strength, modulus of rupture, thickness swelling, and water absorption properties are the function of independent operating factors such as steaming temperature (A_1), steaming time (A_2), hot pressing temperature (A_3), and hot pressing time (A_4). This relation in terms of function representation can be shown as in Eq. (5),

$$Y = f(A_1, A_2, A_3, A_4) + \phi \quad (5)$$

where ϕ represents the error observed in the responses Y. If the expected response is represented by the equation $E(Y) = f(A_1, A_2, A_3, A_4) = \chi$, then the surface represented by $\chi = f(A_1, A_2, A_3, A_4)$ is called the surface response (Montgomery 1999).

The experimental combination for each trial was mixed in order to eliminate the effect of uncontrolled error in operating factors. The output response of each trials of the board making was used to develop an empirical mathematical model that correlates the each characteristics of the board with process operating variables as in Eq. (6),

$$Y = \alpha_0 + \sum_{i=1}^{n} \alpha_i A_i + \sum_{i=1}^{n} \alpha_{ii} A_i^2 + \sum \sum_{j=2\ i<j}^{n} \alpha_{ij} A_i A_j + \sum \sum_{k=3\ i<k}^{n} \alpha_{ik} A_i A_k + \sum \sum_{l=4\ i<l}^{n} \alpha_{il} A_i A_l + \sum \sum_{j<k}^{n} \alpha_{jk} A_j A_k + \sum \sum_{j<l}^{n} \alpha_{jl} A_j A_l + \sum \sum_{k<l}^{n} \alpha_{kl} A_k A_l + \phi \quad (6)$$

where Y is the responses, α_0 the intercept of the model, α_i the linear coefficient, α_{ii} is the quadratic coefficients, α_{ij}, α_{ik}, α_{il}, α_{jk},α_{jl} α_{kl} are the interaction coefficients and A_i A_j A_i, A_j, A_k, A_l are the coded values of the independent operating variables. The total number of binderless particleboard (N) required for the optimization study was given in Eq. (7),

$$N = 2^n + 2n + n_c = 2^4 + 4 \times 2 + 6 = 30 \quad (7)$$

where n is the number of manufacturing variables, and n_c is the number of center point data. The operating factors were varied within the selected range (as given in Table 1) to obtain optimized values for the steaming temperature (A1), steaming time (A2), hot pressing temperature (A3) and hot pressing time (A4) by keeping the hot pressing pressure 12 MPa, average density of the board 0.8 g/cm^3 and moisture content of raw palm trunk particle was maintained at 8%. The desired ranges of the operating variables are defined and coded to lie at ±1 for the factorial points, 0 for center points and ±2 for the axial points.

Table 1. Manufacturing Condition Variables with Corresponding Levels of Binderless Particleboard Manufactured Using Steam Treated Particles Oil Palm Trunk Particles

Parameters	Factor	Variable levels				
		-2	-1	0	1	2
Steaming temperature (°C)	A_1	90	100	110	120	130
Steaming time (min)	A_2	13	25	37.5	50	62.5
Hot pressing temperature (°C)	A_3	160	180	200	220	240
Hot pressing time (min)	A_4	7.5	15	22.5	30	37.5

For mathematical model development through a set of experimental data and analysis of variance (ANOVA) calculation, the statistical software package Design Expert Version 6.0.10 software, Stat-Ease, Inc., USA was used. This software was also enabled to plot regression lines, contour, and response surface plots.

Field Emission Scanning Electron Microscopy (FESEM) and Energy Dispersive X-ray Spectroscopy (EDX)

The FESEM images of raw oil palm trunk waste and optimized binderless particleboard were recorded using a Leo Supra 50 VP Field Emission Scanning Electron Microscope (Carl-Ziess SMT, Oberkochen, Germany) equipped with an Oxford INCA 400 energy dispersive x-ray microanalysis system (Oxford Instruments Analytical, Bucks, U.K.) that can give FESEM and EDX from the same sample. A thin layer of gold was sputter-coated on the samples for charge dissipation during imaging

RESULTS AND DISCUSSION

Based on the sequential model sum of squares, the proposed mathematical models were selected based on the highest order polynomials for which the additional terms were significant and the models were not aliased. For internal bond (IB) strength and modulus of rupture (MOR), the quadratic models were selected as suggested by the rotatable central composite design statistical tool (Table 2).

Table 2. Actual and Coded Parameters for Designed Experiments

Run	Actual parameters				Coded parameters				Y_1 (Mpa)	Y_2 (Mpa)	Y_3 (%)	Y_4 (%)
	A_1	A_2	A_3	A_4	X_1	X_2	X_3	X_4				
1	120	25.0	180	30.0	1	-1	-1	1	0.50	5.42	68.75	102.27
2	120	50.0	180	15.0	1	1	-1	-1	0.45	8.52	64.98	111.13
3	110	37.5	240	22.5	0	0	2	0	0.11	5.61	23.98	111.13
4	100	25.0	180	15.0	-1	-1	-1	-1	0.49	5.16	63.23	102.83
5	110	13.0	200	22.5	0	-2	0	0	0.24	5.04	54.14	80.88
6	130	37.5	200	22.5	2	0	0	0	0.71	10.01	29.97	63.42
7	110	37.5	200	37.5	0	0	0	2	0.45	8.06	27.74	71.57
8	90	37.5	200	22.5	-2	0	0	0	0.17	3.71	32.37	63.41
9	100	25.0	220	30.0	-1	-1	1	1	0.41	4.72	19.51	102.40
10	110	37.5	160	22.5	0	0	-2	0	0.37	4.29	77.78	115.02
11	110	37.5	200	7.5	0	0	0	-2	0.23	4.83	51.37	98.26
12	110	37.5	200	22.5	0	0	0	0	0.23	10.1	36.94	73.57
13	120	50.0	220	30.0	1	1	1	1	0.34	5.72	14.02	52.81
14	120	50.0	220	15.0	1	1	1	-1	0.30	5.81	20.71	53.92
15	110	62.5	200	22.5	0	2	0	0	0.52	8.25	22.34	57.71
16	100	50.0	220	15.0	-1	1	1	-1	0.27	5.43	19.66	58.23
17	100	50.0	180	30.0	-1	1	-1	1	0.40	5.16	64.03	90.14
18	110	37.5	200	22.5	0	0	0	0	0.24	9.87	36.74	73.56
19	120	25.0	180	15.0	1	-1	-1	-1	0.61	8.85	68.25	112.74
20	110	37.5	200	22.5	0	0	0	0	0.23	10.46	36.80	73.37
21	100	50.0	180	15.0	-1	1	-1	-1	0.46	5.24	60.54	99.10
22	110	37.5	200	22.5	0	0	0	0	0.34	10.66	36.64	73.47
23	110	37.5	200	22.5	0	0	0	0	0.25	9.89	36.84	73.47
24	120	25.0	220	30.0	1	-1	1	1	0.53	5.04	12.91	45.29
25	100	25.0	220	15.0	-1	-1	1	-1	0.25	4.97	19.08	148.68
26	100	50.0	220	30.0	-1	1	1	1	0.41	4.82	13.34	37.23
27	120	50.0	180	30.0	1	1	-1	1	0.45	5.69	54.11	86.56
28	110	37.5	200	22.5	0	0	0	0	0.29	10.55	36.84	73.47
29	120	25.0	220	15.0	1	-1	1	-1	0.23	5.06	22.68	48.60
30	100	25.0	180	30.0	-1	-1	-1	1	0.25	5.19	30.84	28.93

A_1= steaming temperature (°C), A_2= steaming time (min), A_3= hot pressing temperature (°C), A_4= hot pressing time (min); X_1 = steaming temperature X_2 = steaming time X_3 = hot pressing temperature X_4 =hot pressing time, Y_1 = Internal bond strength Y_2 = Modulus of rupture Y_3= Thickness swelling Y_4= Water absorption.

The design of proposed experiment is given in Table 2, together with the experimental results. The physical and mechanical responses were expressed in terms of internal bond (IB) strength, modulus of rupture (MOR), thickness swelling (TS), and water absorption (WA). The regression analysis was performed to fit the responses such as internal bond (IB) strength, modulus of rupture (MOR), thickness swelling (TS), and water absorption (WA). The mathematical model represents internal bond strength (Y_1), modulus of rupture (Y_2), thickness of swelling (Y_3), and water absorption, (Y_4) as a function of steaming temperature (A_1), steaming time (A_2), hot pressing temperature (A_3), and hot pressing time (A_4). The mathematical model in terms of coded factors is given in Eqs. 8 through 11.

$$Y_1 = 0.26 + 0.065A_1 + 0.015A_2 - 0.058A_3 + 0.028A_4 + 0.052A_1^2 + 0.038A_2^2 + 1.981\times10^{-3}A_3^2 + 0.027A_4^2 - 0.029A_1A_2 - 0.022A_1A_3 + 0.014A_1A_4 - 6.25\times10^{-4}A_2A_3 + 6.25\times10^{-4}A_2A_4 + 0.066A_3A_4 \quad (8)$$

$$Y_2 = 10.25 + 0.92A_1 + 0.36A_2 - 0.21A_3 + 0.049A_4 - 0.96A_1^2 - 1.03A_2^2 - 1.43A_3^2 - 0.94A_4^2 + 0.048A_1A_2 - 0.38A_1A_3 - 0.34A_1A_4 + 0.13A_2A_3 + 3.750\times10^{-3}A_2A_4 + 0.33A_3A_4 \quad (9)$$

$$Y_3 = 39.95 + 1.31A_1 - 2.39A_2 - 14.93A_3 - 4.54A_4 \quad (10)$$

$$Y_4 = 79.44 - 2.26A_1 - 6.25A_2 - 8.10A_3 - 10.12A_4 + 5.85A_1A_2 - 14.85A_1A_3 + 6.92A_1A_4 - 11.43A_2A_3 + 4.90A_2A_4 + 2.89A_3A_4 \quad (11)$$

A positive sign before the co-efficient of variable terms indicates a synergistic effect, whereas a negative sign indicates an antagonistic effect. The proposed mathematical model fitting ability with the obtained experimental data was judged from their correlation coefficients and statistical significance test (prob>F). The correlation coefficients and "prob>F" of the proposed mathematical model for the responses were estimated using a multiple regression analysis included in the response surface methodology technique. For all the four mathematical models (Eqs. 8 to 11) the "prob>F" was less than 0.05, which shows that the proposed models were significant. Other model fitting tests such as sum of squares, mean squares, and F-values are shown in Table 3. The model predicted values through Eqs. 8 to 11 and the experimentally calculated values of the responses are given in Table 4. The authenticities of the developed mathematical models were evaluated based on the adequate precision, standard deviation value, F-value, adjusted R^2, and coefficient of variation (CV). The desired adequate precision ratio was 4.0, whereas the adequate precision ratio for all the responses were found more than 6.167, which suggested that the model provided adequate signal to be used to navigate in the design space. The standard deviations in the responses are within the statistically acceptable range. The model F-values for internal bond strength, modulus of rupture, thickness swelling, and water absorption were 2.81, 5.41, 27.14, and 2.75 which indicate that there was a chance that the model F-value was due to noise of only 2.82%, 0.12%, 0.01%, and 2.78%, respectively.

Table 3. Analysis of Variance (ANOVA)

Source		IB strength (Y_1)	MOR (Y_2)	TS (Y_3)	WA (Y_4)
Model	Sum of squares	0.41	127.53	8752.55	12537.00
	DF	14	14	4	10
	Mean square	0.03	9.11	2188.14	1253.70
	F value	2.81	5.41	27.1	2.75
	Prob > F	0.0282[a]	0.0012 [a]	0.0001 [a]	0.0278 [a]
Residual	Sum of squares	0.16	25.26	2015.33	8666.09
	DF	15.00	15.00	25.00	19
	Mean square	0.010	1.68	80.61	456.05
Lack of fit	Sum of squares	0.15	24.66	2015.27	8665.01
	DF	10	10	20	14
	Mean square	0.015	2.47	100.76	618.93
	F Value	7.69	20.60	9688.81	1.157×10^5
	Prob > F	0.0181 [a]	0.0019 [a]	<0.0001[a]	<0.0001 [a]
Pure error	Sum of squares	9.533E-003	0.60	0.05	0.27
	DF	5	5	5	5
	Mean square	1.907E-003	0.12	0.01	0.00
Std.dev.		0.10	1.30	8.98	21.36
R^2		0.72	0.83	0.8128	0.5913
Adjusted R^2		0.47	0.68	0.7829	0.3762
Predicted R^2		-0.51	0.06	0.7085	-0.5482
Adeq precision		6.167	6.785	20.026	7.207
Mean		0.36	6.74	38.57	79.44
C.V		28.53	19.26	23.28	26.88
Press		0.85	143.37	3139.05	32826.05

[a] Models are statistically significant ($p < 0.05$), IB = Internal bond strength, MOR= Modulus of rupture, TS= Thickness swelling (%), WA= Water absorption

Table 4. Actual and Predicted Values of Response Parameters of Binderless Particleboard Using Steam Treated Oil Palm Trunk Particles at their Corresponding Manufacturing Factors

Run no.	Parameter in uncoded levels				IB strength (MPa)		MOR (MPa)		TS (%)		WA (%)	
	A_1	A_2	A_3	A_4	Y_1		Y_2		Y_3		Y_4	
					Actual	Predicted	Actual	Predicted	Actual	Predicted	Actual	Predicted
1	120	25.0	180	30.0	0.50	0.52	5.42	6.36	68.75	56.08	102.27	78.10
2	120	50.0	180	15.0	0.45	0.53	8.52	8.35	64.98	60.39	111.13	112.38
3	110	37.5	240	22.5	0.11	0.15	5.61	4.18	23.98	13.26	111.13	63.25
4	100	25.0	180	15.0	0.49	0.36	5.16	4.61	63.23	62.54	102.83	100.44
5	110	13.0	200	22.5	0.24	0.38	5.04	5.66	54.14	43.25	80.88	91.69
6	130	37.5	200	22.5	0.71	0.60	10.01	8.34	29.97	41.19	63.42	74.93
7	110	37.5	200	37.5	0.45	0.43	8.06	6.02	27.74	29.50	71.57	59.20
8	90	37.5	200	22.5	0.17	0.34	3.71	4.67	32.37	35.96	63.41	83.96
9	100	25.0	220	30.0	0.41	0.32	4.72	5.30	19.51	16.76	102.40	92.94
10	110	37.5	160	22.5	0.37	0.39	4.29	4.01	77.78	75.28	115.02	95.64
11	110	37.5	200	7.5	0.23	0.31	4.83	6.16	51.37	47.65	98.26	99.70
12	110	37.5	200	22.5	0.23	0.26	10.10	10.25	36.94	38.57	73.57	79.45
13	120	50.0	220	30.0	0.34	0.46	5.72	6.68	14.02	14.61	52.81	46.99
14	120	50.0	220	15.0	0.30	0.24	5.81	6.76	20.71	23.68	53.92	37.84
15	110	62.5	200	22.5	0.52	0.45	8.25	6.94	22.34	33.81	57.71	66.95
16	100	50.0	220	15.0	0.27	0.24	5.43	4.90	19.66	21.07	58.23	74.18
17	100	50.0	180	30.0	0.40	0.35	5.16	4.93	64.03	48.70	90.14	59.25
18	110	37.5	200	22.5	0.24	0.26	9.87	10.25	36.74	38.54	73.56	79.45
19	120	25.0	180	15.0	0.61	0.56	8.85	7.78	68.25	65.15	112.74	100.08
20	110	37.5	200	22.5	0.23	0.26	10.46	10.25	36.80	38.57	73.37	79.45
21	100	50.0	180	15.0	0.46	0.45	5.24	4.98	60.54	57.77	99.10	89.32
22	110	37.5	200	22.5	0.34	0.26	10.66	10.25	36.64	38.57	73.47	79.45
23	110	37.5	200	22.5	0.25	0.26	9.89	10.25	36.84	38.57	73.47	79.45
24	120	25.0	220	30.0	0.53	0.49	5.04	5.60	12.91	19.38	45.29	60.85
25	100	25.0	220	15.0	0.25	0.16	4.97	4.02	19.08	25.84	148.68	131.04
26	100	50.0	220	30.0	0.41	0.40	4.82	6.19	13.34	12.00	37.23	55.67
27	120	50.0	180	30.0	0.45	0.49	5.69	6.94	54.11	51.31	86.56	109.98
28	110	37.5	200	22.5	0.29	0.26	10.55	10.25	36.84	38.57	73.47	79.45
29	120	25.0	220	15.0	0.23	0.27	5.06	5.69	22.68	28.45	48.60	71.28
30	100	25.0	180	30.0	0.25	0.26	5.19	4.54	30.84	53.46	28.93	50.79

A_1= steaming temperature (°C), A_2= steaming time (min), A_3= hot pressing temperature (°C), A_4= hot pressing time (min), IB = Internal bond strength (MPa), MOR= Modulus of rupture (MPa), TS= Thickness swelling (%), WA= Water absorption (%)

Effect of Manufacturing Conditions on Internal Bond Strength

The internal bond strength was measured using a formula related to the breaking load of perpendicular tensile strength to the board (JIS-A 5908, 2003). The results indicated that the bonded areas were the actual tested areas. The internal bond strength obtained from the tested specimens was evaluated from the bonded areas. The three-dimensional response surface plots display the effect of manufacturing variables on internal bond strength, as shown in Fig. 1a-f. All three dimensional surfaces shown in figures are quadratic in nature with a different pattern of manufacturing parameters effect.

Figure 1a shows the effect of steaming time and temperature of raw oil palm trunk waste on binderless particleboard internal bond strength. A quadratic nature of the response surface plot was observed, as represented in the figure. With the increase of steaming time and steaming temperature the internal bond strength of the binderless particleboard was found to increase. From the individual effects of steaming time and steaming temperature, it was observed that with the increase of either of the two parameters the internal bond strength rose, but the steaming temperature had a more pronounced effect on the internal bond strength of the binderless particleboard compared to steaming time. Hence internal bond strength can be expressed as the quadratic function of steaming time and steaming temperature. Figure 1b expresses the effect of hot pressing temperature and steaming temperature on internal bonding strength of binderless particleboard. It was observed that with the rise of hot pressing temperature from 180 °C to 220 °C there was no change in the internal bond strength of the binderless particleboard, but with the rise of steaming temperature from 100 °C to 120 °C the internal bond increased from 0.24 MPa to 0.46 MPa. Combined effects of both parameters led to increases in the internal bond strength but not as much as steaming temperature alone can do. Fig. 1c represents the response surface plot that indicated the effect of hot pressing time and steaming temperature. It can be seen from the figure that an individual rise in each factor gave only little increment in the IB strength of the binderless particleboard, but the combined effect of both factors markedly increased the internal bond strength of the binderless particleboard up to 0.45 MPa.

The response surface plot in Fig. 1d suggests that an increase in hot pressing temperature did not have any role in an increase of the internal bond strength, but an increase in steaming time increased the internal bond strength of the binderless particleboard to a maximum value. The increment in the internal bond strength of the binderless particleboard due to a combined effect of steaming time and hot pressing temperature was less than the steaming time alone. The response surface plot in Fig. 1e suggests that the increase in the hot pressing time and steaming time increases the internal bond strength, but hot pressing time yielded a more pronounced effect. The combined effect of the manufacturing variables on the internal bond strength of the binderless particleboard was found to be more effective compared to each individual effect. The response surface plot in Fig. 1f represents the effect of hot pressing time and hot press temperature on internal bond strength of the binderless particleboard. It can be seen from the figure that with the rise of hot press temperature from 180 °C to 220 °C the internal bond strength of the particleboard was decreased, whereas with the rise of hot pressing time from 15 min to 30 min, the internal bond strength increased. The overall effect of both the parameters is guided by the hot press time, hence an increase in internal bond strength was recorded.

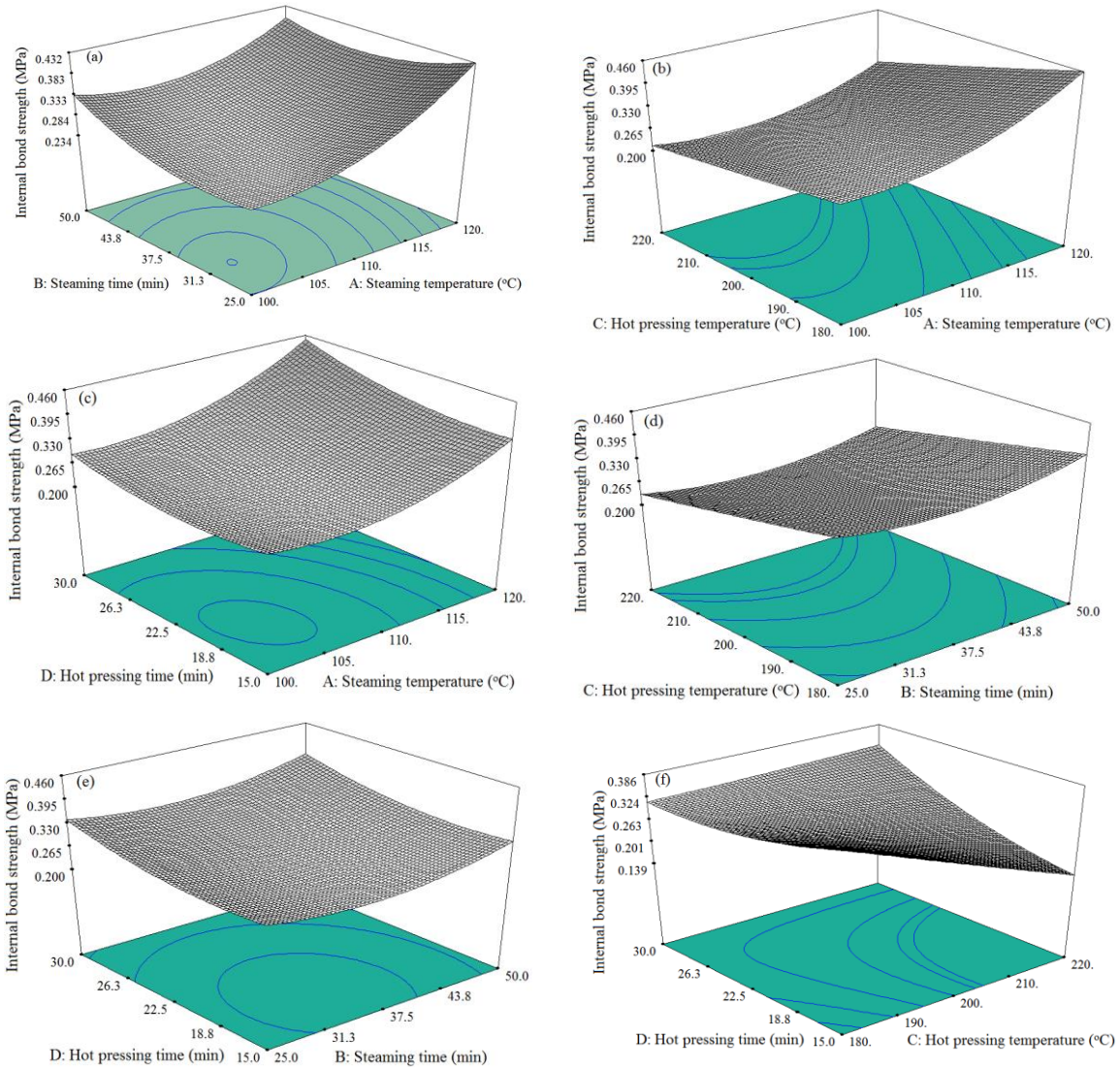

Fig. 1. Internal bond strength relationship between factors of (a) steaming temperature and steaming temperature (b) hot pressing temperature and steaming temperature (c) hot pressing time and steaming temperature (d) hot pressing temperature and steaming time (e) hot pressing time and steaming time and (f) hot pressing time and hot pressing temperature

The adhesion force in binderless particleboard made from steam-treated oil palm trunk can be explained based on intermolecular hydrogen bonding between the cellulose and lignin molecules. As the celluloses and lignins are the basic unit of oil palm trunk biomass, it seems that the hydrogen bonding between these two molecules occurred during board making. The intermolecular hydrogen bonding occurs when an atom of hydrogen is attracted by the more electronegative atoms such as oxygen, nitrogen, and fluorine; in case of cellulose and lignin the probable forming of hydrogen bonding is between hydrogen and oxygen. The strength of the hydrogen bonding depends upon the bond angle and bond length (Grabowski 2001). The hydrogen bond strength varies with the bond angle relative to the O-H covalent bond. If the hydrogen bond is close to a straight line (180°), then the bond strength solely depends upon the length of the bond. The increasing or decreasing of the bond strength is linearly guided by the shorter and larger bond lengths respectively. The atomic charges of oxygen and hydrogen atoms effectively increase the response to

polarization in the molecule. The hydrogen bond length increases with an increase in hot pressing temperature and decreases with increasing the applied pressure (Dougherty 1998). Figure 2 shows the possible mechanism of the hydrogen bonding in oil palm trunk binderless particleboards. The terminal –OH groups of cellulose and lignin are mainly involved in formation of hydrogen bonding. In the cellulose chain, the anhydroglucose unit adopts the chair configuration with the hydroxyl groups located at the equatorial position and the hydrogen atoms in the axial positions. Every unit in the cellulose chain is rotated at 180° around the main axis that gives unstrained linear configuration with minimum hindrances (Sihtola and Neimo 1975). All significant chemical reactions occur at glycosidic linkage and hydroxyl groups. The coniferyl alcohol unit of lignin joined with the equatorial hydroxyl group with hydrogen bonding and during hot pressing, the number of hydrogen bonding increases between the cellulose of lignin units as represented in Fig. 2. Overend *et al.* (1987) reported that 10 to 15% of the original lignin is water soluble during steam treatment, and the hemicellulose was hydrolysed at a low rate during steaming temperature.

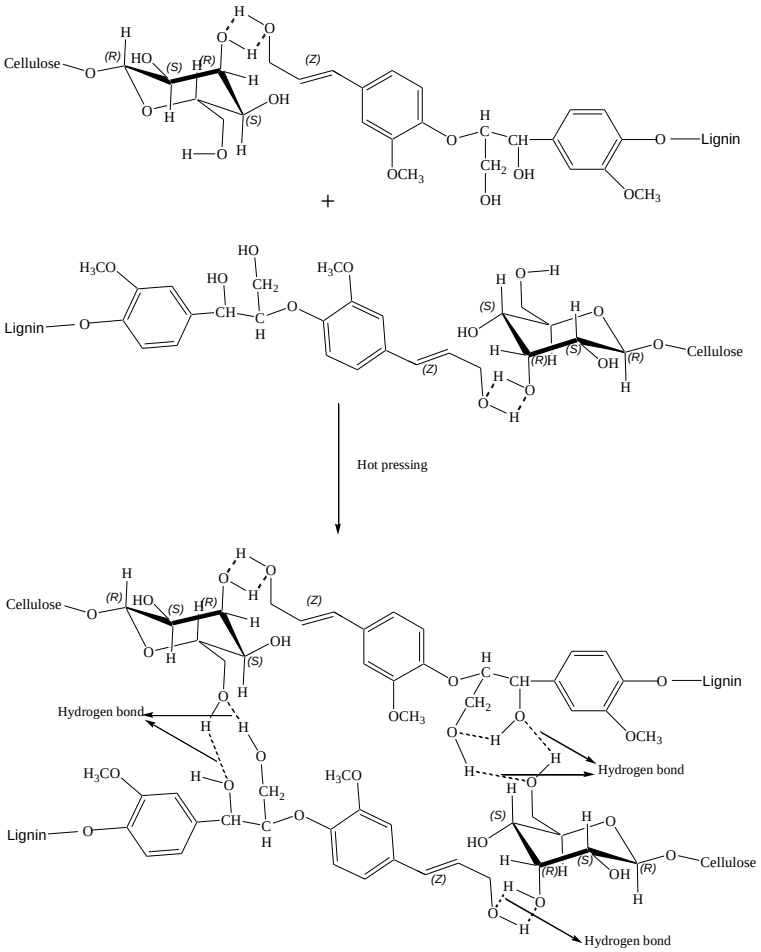

Fig. 2. Hydrogen bond between oil palm trunk particles of binderless particleboard

The role of water molecules during board making cannot be denied, since the oil palm trunk particle contains around 7% moisture. If moisture falls below 3%, one will get a weaker board, and excess water is also detrimental to the strength of the binderless

particle boards. The moisture between 7 and 10% of the oil palm trunk waste particle is ideal to obtain maximum board strength, because the water molecules in this range of moisture likely contribute to hydrogen bonding in the binderless particle board.

Effect of Manufacturing Conditions on the Modulus of Rupture (MOR)

The modulus of rupture is a crucial parameter to decide the mechanical strength of the particle boards. It reflects the maximum load-bearing capacity of the board in bending and is proportional to maximum moment borne by the sample specimen (JIS-A 5908, 2003). In this study the four manufacturing variables of steaming temperature, steaming time, hot pressing temperature, and hot pressing time were considered. The effects of these manufacturing variables on the modulus of rupture followed quadratic mathematical model and are shown in Fig. 3a-f. The three dimensional (3D) response surface plots were used to display the consequence of different manufacturing variables on the modulus of rupture (MOR). The response surface plots indicated that with the rise of steaming temperature, the MOR initially rises and reaches maximum at nearly average value of the manufacturing variable, then starts decreasing. From Fig. 3a-f, dome-shaped response surface plots can be seen for all manufacturing variables. This nature of the plot suggested that the maximum MOR was in the middle values of the steaming temperature, steaming time, hot pressing temperature, and hot pressing time. The results indicated that the maximum value of MOR lies within the range of selected manufacturing variables ranges.

Effect of Manufacturing Conditions on Thickness Swelling (TS)

The thickness swelling of the board was measured after applying different manufacturing variables of the board making. According to the proposed model, the thickness swelling of the binderless particleboard linearly depends on manufacturing variables such as steaming temperature, steaming time, hot pressing temperature, and hot pressing time. Figure 4a-f represents the response surface linear plots for different combination of manufacturing variables. The thickness swelling data clearly indicates the effect of steaming time and steaming temperature on thickness swelling. The increase of steaming time marginally decreases the thickness swelling, while with the rise of steaming temperature increased the thickness swelling. The reason behind the increase of the thickness swelling of binderless particleboard was the water soluble nature of hemicellulose molecules at increasing temperature. When we maintained the steam at low temperature and steamed the oil palm trunk waste particles for a long time the resultant particleboard showed low thickness swelling because low temperature of steam was not favorable for water solubility of hemicelluloses molecules. The effect of hot pressing temperature and steaming temperature on thickness swelling of binderless particleboard is shown in Fig. 4b. The hot pressing temperature makes the surface of board compact by removing the void space, and lignin melts in the temperature range 180 to 220 °C (Brebu and Vasile 2010) to fill the spaces. As a result, during soaking the surface restricts the entry of water molecules into the pores, thus reducing the thickness swelling.

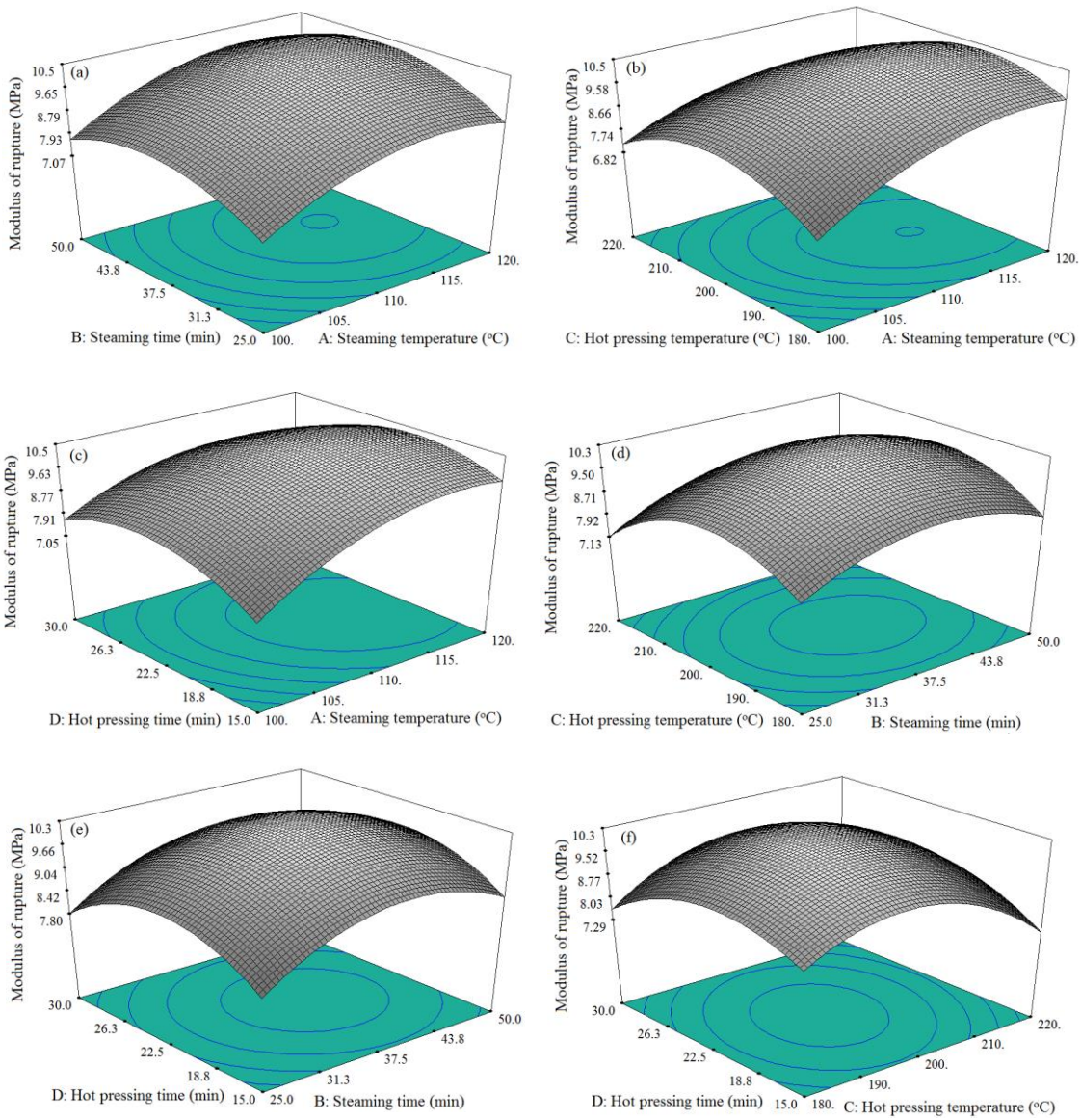

Fig. 3. Modulus of rupture (MOR) relationship between factors of (a) steaming temperature and steaming temperature, (b) hot pressing temperature and steaming temperature, (c) hot pressing time and steaming temperature, (d) hot pressing temperature and steaming time, (e) hot pressing time and steaming time, and (f) hot pressing time and hot pressing temperature

Figure 4c compares the effect of hot pressing time and steaming temperature during board making. The increase of hot pressing time decreases the thickness swelling of the oil palm trunk waste binderless particleboards. The reason is probably the long duration of hot pressing, changing the surface of the board such that it can effectively resist the entry of water molecules into the bulk of the board. Figure 4d depicts the combined effect of hot pressing temperature and steaming time. It can be inferred from the figure that at a higher value of hot pressing temperature and steaming time the thickness swelling reached 19%, whereas at a lower value of these parameters it was 68% while keeping the other manufacturing variables such as steaming temperature and hot pressing time at its average values.

The combined effect of hot pressing time and steaming time on the thickness swelling is shown in Fig. 4e. It can be seen from the response surface plot, at the average

value of steaming temperature and hot pressing temperature the increase or decrease of duration did not have much effect on thickness swelling properties of the binderless particleboard. Figure 4f shows the combined effect of hot pressing time and hot pressing temperature. The effectiveness of these two manufacturing variables on dimensional stability has been proven by the obtained results. At lower values of hot pressing time (15 min) and hot pressing temperature (180 °C), the thickness swelling was 65%, and it was reduced to 12.91% when hot pressing time and temperature increased to 30 min and 220 °C, respectively.

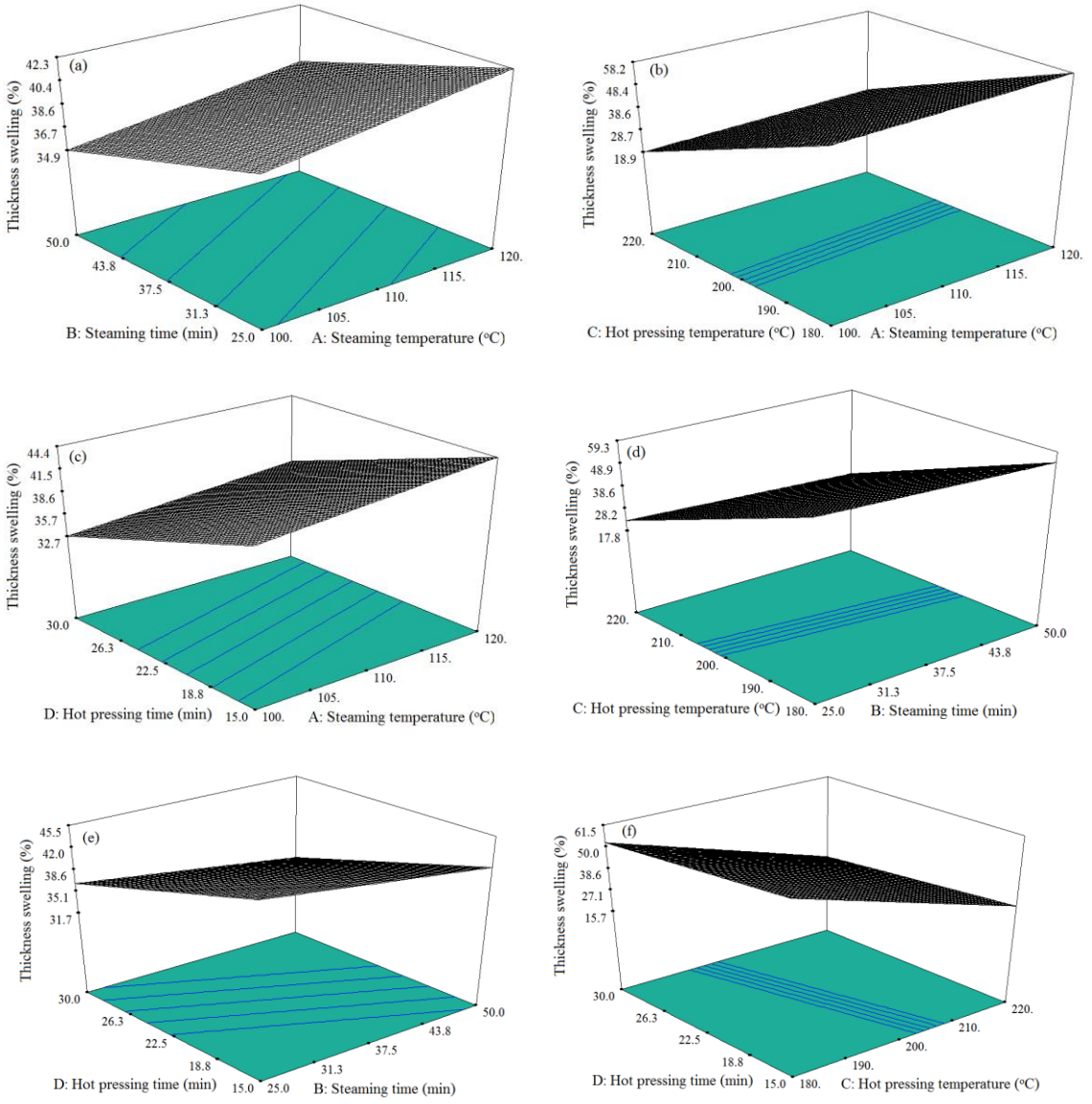

Fig. 4. Thickness swelling (TS) relationship between factors of (a) steaming temperature and steaming temperature, (b) hot pressing temperature and steaming temperature, (c) hot pressing time and steaming temperature, (d) hot pressing temperature and steaming time, (e) hot pressing time and steaming time, and (f) hot pressing time and hot pressing temperature

Effect of Manufacturing Conditions on Water Absorption (WA)

The test specimens with dimensions 5 cm x 5 cm x 0.5 cm were cut from the board with an average density 0.8 g/cm^3 made by various manufacturing conditions from oil palm trunk waste. The effect of manufacturing variables on the water absorption property was evaluated using a rotatable central composite design (RCCD). The dependency of water absorption capability on selected manufacturing variables was found to follow a non-linear two factorial interaction model. The three-dimensional response surface plots displaying the effect of different combinations of manufacturing variables on water absorption capability are shown in Fig. 5a-f. The interaction of steaming time and steaming temperature gave a twisted net pattern of response surface plot, as shown in Fig. 5a. The rise of steaming time and steaming temperature decreases the water absorption property of the board. The low water absorption capability at high values of steaming time and steaming temperature was probably due to decreasing void spaces in the surface and bulk of board caused by long time steaming at elevated temperature. Similarly, increase in hot pressing temperature decrease the void spaces. Hence, increasing the hot pressing temperature and steaming temperature during the board manufacturing process gave the low water absorbing capacity to the board, as displayed in Fig. 5b. The combined effect of hot pressing time and steaming temperature, as shown in Fig. 5c, with the rise of these two manufacturing variables during board making, gives the resultant board decreasing water absorption capability. The reason is the same as stated in the case of hot pressing temperature and steaming temperature. It was found that the water absorption decreased at the two extremes of the combined variable range, as shown in Fig. 5d. In Fig. 5e we compared the duration of hot pressing and steaming treatments by keeping the hot pressing temperature and steaming temperature at 200 and 110 °C, respectively. It was found that hot pressing duration had a more pronounced effect on decreasing the water absorption property of the board compared to steaming duration of oil palm trunk waste. Figure 5f gives information about the variation of hot pressing time and hot pressing temperature on water absorption property when steaming time and steaming temperature were fixed at 37.5 min and 110 °C. It was observed that the rising of either of these two variables decreases the water absorption capability of the particleboard. The increase in hot pressing time alone was found effective enough to decrease water absorption capability of the oil palm trunk waste binderless particleboard.

Response Surface Methodology Optimization of Board Making

The desirability function is generally recommended to optimize the processes which have two or more responses. The desirability function combines multiple responses into one function and the function ranges between 0 and 1. The desirability function 0 indicates that responses are unacceptable and 1 indicates that all process characteristics responses are possible. The net desirability value is a geometric mean of the individual desirability functions (Grahovac *et al.* 2012). The goal of optimization in this experiment was to find the optimum manufacturing variables for getting desired response in terms of high internal bond strength, high modulus of rupture, low thickness of swelling, and low water absorption capability of boards. At these conditions the desirability achieved was 0.687, and the optimum values of each manufacturing factors and their responses are reported in Table 5. Under optimized conditions of manufacturing variables we prepared oil palm trunk waste binderless particle board to compare the predicted response results with the experimentally achieved response results. It was found that the difference between the predicted and experimentally achieved values were less than 10%. Under optimized

conditions, the IB strength and MOR were 0.49 and 8.18, MPa respectively. These readings met the JIS standard in which the minimum requirement for IB and MOR were 0.3MPa (Type 18) and 8.0 MPa (Type 8), respectively. The TS and WA were 22.00 % and 51.43 %, respectively and gave satisfactory results.

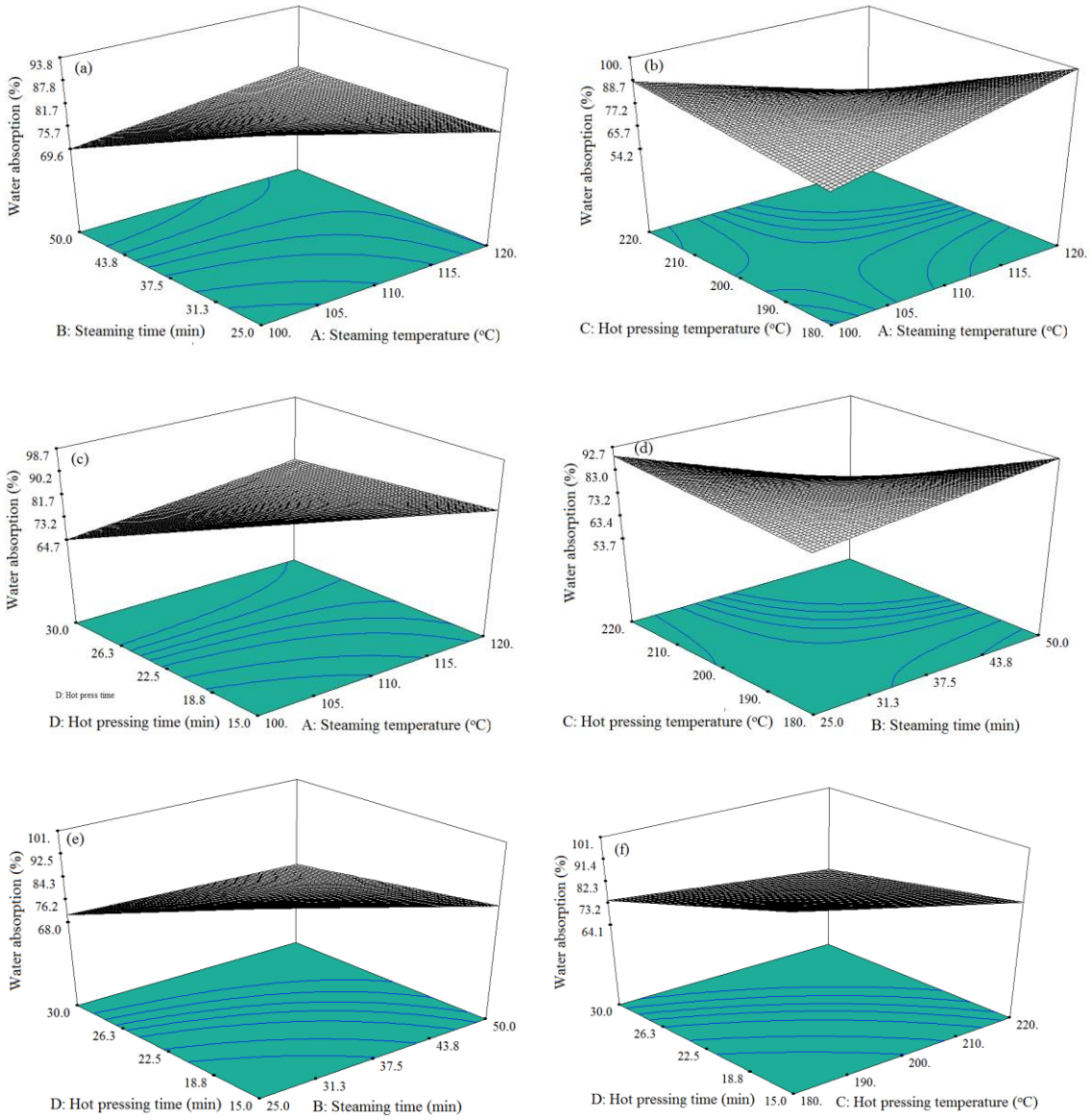

Fig. 5. Water absorption (WA) relationship between factors of (a) steaming temperature and steaming temperature (b) hot pressing temperature and steaming temperature (c) hot pressing time and steaming temperature (d) hot pressing temperature and steaming time (e) hot pressing time and steaming time and (f) hot pressing time and hot pressing temperature

Table 5. A Set of Optimum Solution Suggested by the Design Expert Software

Parameters				Responses								Desirability
A_1	A_2	A_3	A_4	IB (MPa)		MOR (MPa)		TS (%)		WA (%)		
				Obtained	Predicted	Obtained	Predicted	Obtained	Predicted	Obtained	Predicted	
120	46	215	29	0.49	0.44	8.18	7.85	22.00	20.00	51.43	55.66	0.687

A_1= steaming temperature (°C), A_2= steaming time (min), A_3= hot pressing temperature (°C), A_4= hot pressing time (min)

FESEM and EDX of Optimized Binderless Particle Board

Imaging using a Field Emission Scanning Electron Micrograph (FESEM) has become an established technique for surface morphological study of many biomass waste materials. In this study, the FESEM method was used to examine surface morphology of oil palm trunk waste particles after steaming and after making it into binderless particleboard. The FESEM at optimized condition of oil palm trunk waste particles steamed at 120 ˚C for 48.7 min was taken at magnifications 500X, as shown in Fig. 6a.

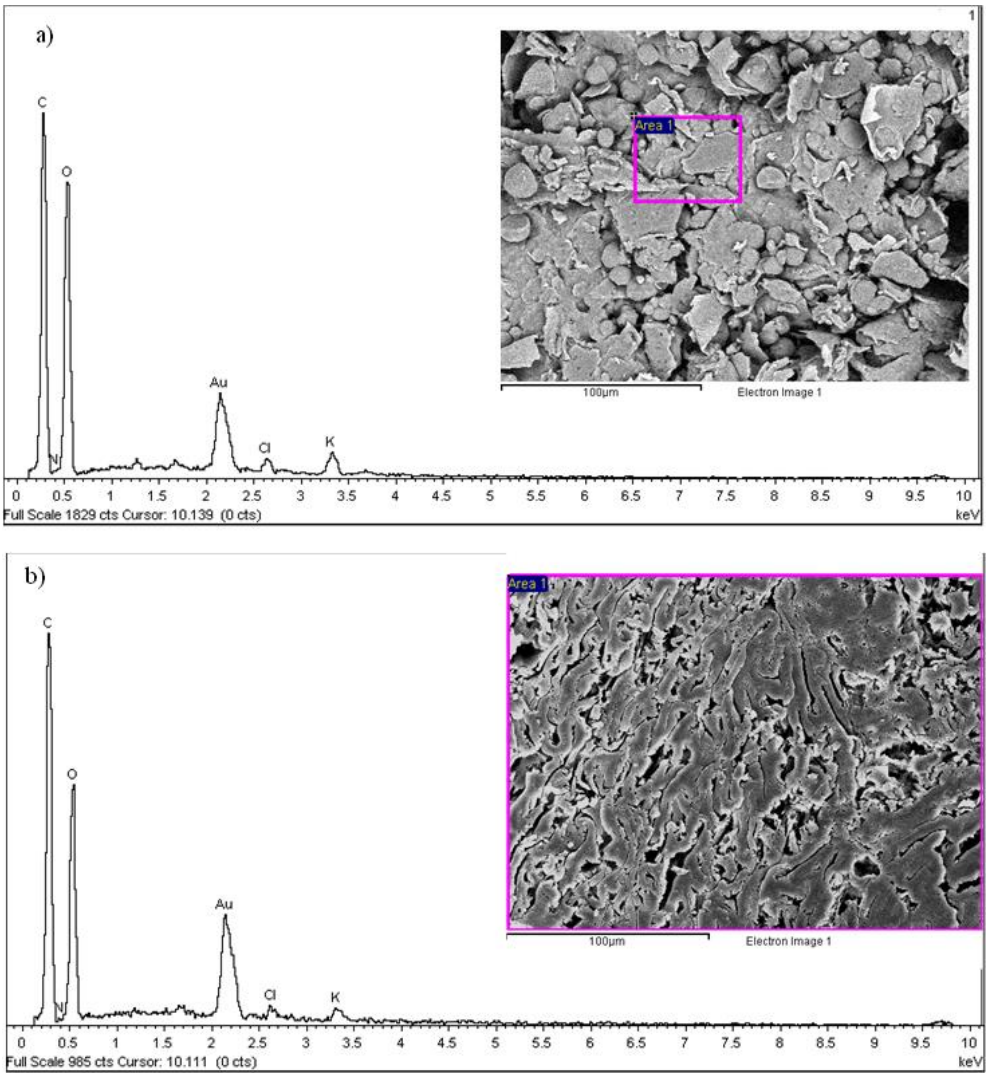

Fig. 6. EDX spectra of a) steam-treated oil palm trunk particles b) binderless particleboard panel

The figure shows many starch granules present after steaming, and all particles were of different sizes. The FESEM of optimized oil palm trunk waste binderless particleboard at magnifications 500X is represented in Fig. 6b. Particles were compressed and bonded together and no starch granules could be seen after hot pressing. The energy dispersive x-ray (EDX) spectroscopy was used to analyze the elemental composition of oil palm trunk waste before and after board making. The elemental composition of the surface of oil palm trunk waste was not changed after board making, as presented in Table 6. A small increase in carbon percentage was due to the loss of some volatile nitrogen, chlorine, potassium, and oxygen compounds during hot pressing.

Table 6. Percentage Weight of Elements in Steam Treated Particles of Oil Palm Trunk Particles and Binderless Particleboard Panel

Element	Weight (%)	
	Before board making	After board making
C	50.57	56.57
N	3.28	1.85
O	44.74	40.65
Cl	0.5	0.38
K	0.91	0.54

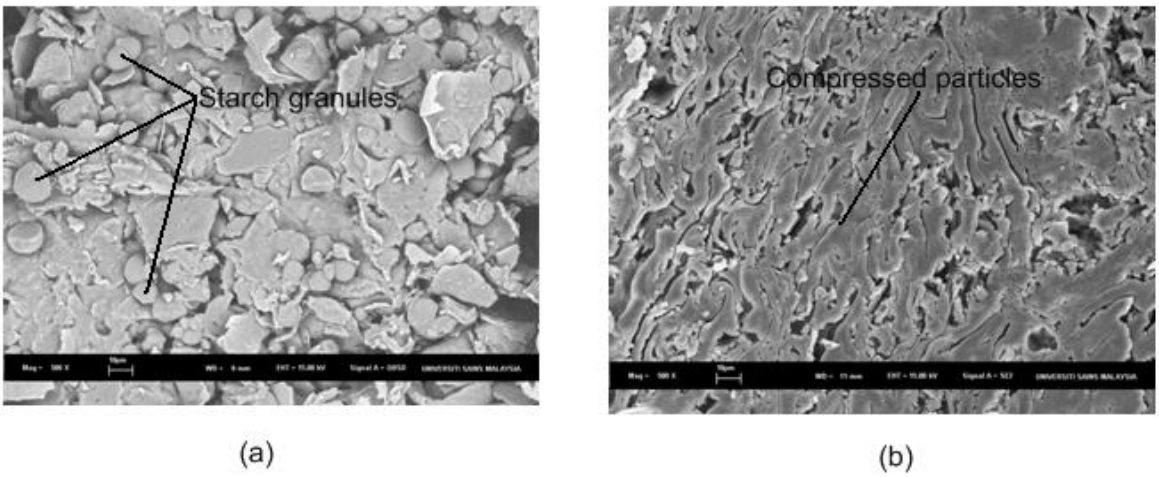

Fig. 7. Field Emission Scanning Electron Micrograph of (a) optimum condition oil palm trunk particles steamed at 120 ˚C for 45 min (magnifications 500X) (b) optimum condition oil palm trunk binderless particleboard after hot pressing at 215 ˚C for 30 min (magnifications 500X)

The thermogravimetric analysis (TGA) curves as shown in Fig. 8 displayed weight loss of the raw oil palm trunk, steam-treated oil palm trunk, and oil palm trunk binderless particleboard at varying temperature. The weight loss values of 8.77%, 7.63%, and 7.15% at temperature 130.6 °C, 130.7 °C, and 149.4 °C, respectively. These initial weight losses correspond to moisture loss. All forms of oil palm trunk had almost the same moisture content at room temperature. With a further rise of temperature to around 297.3 °C for raw

oil palm trunk particles, at 302.9 °C for steam-treated oil palm trunk particles and at 303.8 °C for oil palm trunk binderless particleboard, the additional weight losses were observed to be around 26.06%, 32.47% and 26.22%, respectively. In the temperature range of 200 to 300 °C, the weight loss was probably due to decomposition of cellulose and lignin (Brebu and Vasile 2010).

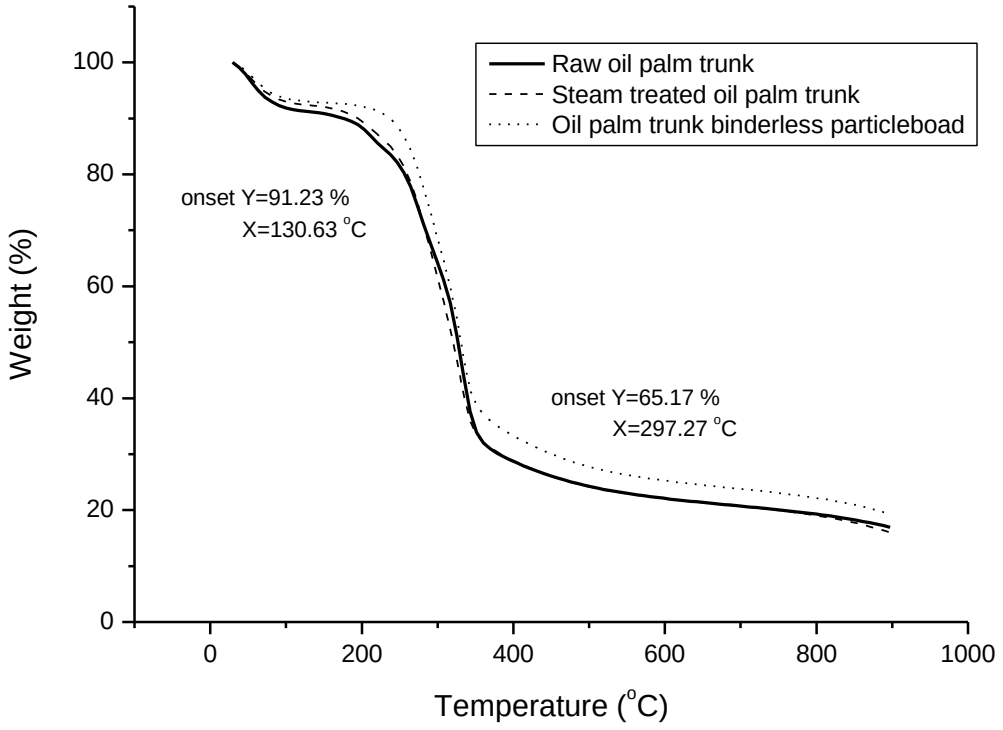

Fig. 8. TGA plot of raw oil palm trunk, optimum condition oil palm trunk particles steamed at 120 ˚C for 45 min and optimum condition oil palm trunk binderless particleboard after hot pressing at 215 ˚C for 30 min

CONCLUSIONS

1. High-performance binderless particleboard can be manufactured with proper manufacturing conditions using steamed oil palm trunk waste as the raw material.
2. The mechanical properties improved significantly with increasing time of steaming of the raw oil palm trunk waste and hot pressing temperature during board formation, but will decrease at long duration of steaming time and high hot pressing temperature.
3. An increase in hot pressing time contributes to less thickness swelling and better dimensional stability. The optimized value of manufacturing variables were 120 °C, 46 min, 215 °C, and 29 min for steaming temperature, steaming time, hot pressing temperature, and hot pressing time, respectively.

4. From actual experiments, at optimized conditions, the binderless particleboard has internal bond strength, 0.49 MPa; modulus of rupture, 8.18 MPa; thickness swelling, 22%; and water absorption, 51.43%.
5. In EDX, a small change in carbon percentage could be due to loss of some volatile nitrogen, chlorine, potassium, and oxygen compounds during hot pressing. The FESEM showed the presence of starch granules after the steaming process; such particles could not be seen after the particles had been subjected to hot pressing.

ACKNOWLEDGMENTS

The authors would like to acknowledge Ministry of Higher Education, Malaysia for the Exploratory Research Grant Scheme (203/PTEKIND/6730054) and MyBrain15 scholarship to W. N. A. W. Nadhari, respectively.

REFERENCES CITED

Ahmadi, M., Vahabzadeh, F., Bonakdarpour, B., Mofarrah, E., and Mehranian, M. (2005). "Application of the central composite design and response surface methodology to the advanced treatment of olive oil processing wastewater using Fenton's peroxidation," *J. Hazard. Mater.* 123, 187-195.

Brebu, M., and Vasile, C. (2010). "Thermal degradation of lignin - A review," *Cell. Chem. and Tech.* 44, 353-363.

Chang, J. I., Lin, J. J., Huang, J. S., and Chang, Y. M. (2006). "Recycling oil and steel from grinding swarf," *Resour. Conserv. Recy.* 49, 191-201.

Dougherty, R. C. (1998). "Temperature and pressure dependence of hydrogen bond strength: A perturbation molecular orbital approach," *J. Chem. Phys.* 109, 7372-7378.

Grabowski, S. J. (2001). "A new measure of hydrogen bonding strength ab initio and atoms in molecules studies," *Chem. Phys. Lett.* 338, 361-366.

Grahovac, J., Dodić, J., Jokić, A., Dodić, S, and Popov, S. (2012). "Optimization of ethanol production from thick juice: A response surface methodology approach," *Fuel* 93, 221-228.

Hashim, R., Hamid, S. H. A., Sulaiman, O., Ismail, N., Ibrahim, M. H., and Jais, H. (2009). "Extractable formaldehyde from waste medium density fibreboard," *J. Trop. For. Sci.* 21, 25-33.

Hashim, R., Nadhari, W. N. A. W., Sulaiman, O., Kawamura, F., Hiziroglu, S., Sato, M., Sugimoto, T., Tay, G. S., and Tanaka, R. (2011). "Characterization of raw materials and manufactured binderless particleboard from oil palm biomass," *Mater. Design* 32, 246-254.

Hashim, R., Saari, N., Sulaiman, O., Sugimoto, T., Hiziroglu, S., Sato, M., and Tanaka, R. (2010). "Effect of particle geometry on the properties of binderless particleboard manufactured from oil palm trunk," *Mater. Design* 31, 4251-4257.

JIS- A 5908, (2003). Particleboards. Japanese Standards Association, 1-24 Akasaka, 4 Minato-ku, Tokyo 107, Japan.

Laemsak, N., and Okuma, M. (2000). "Development of boards made from oil palm frond Ih properties of binderless boards from steam-exploded fibers of oil palm frond," *J. Wood Sci.* 46, 322-326.

Mancera, C., El Mansouri, N.-E., Pelach, M. A., Francesc, F., and Salvadó, J. (2012). "Feasibility of incorporating treated lignins in fiberboards made from agricultural waste," *Waste Manage.* 32, 1962-1967.

Montgomery, D. C. (1999). "Experimental design for product and process design and development," *Journal of the Royal Statistical Society: Series D (The Statistician)* 48, 159-177.

Overend, R., Chornet, E., and Gascoigne, J. A. (1987). "Fractionation of lignocellulosics by steam-aqueous pretreatments," *Phil. Trans. R. Soc. Lond*. 321, 523-536.

Pandey, A., and Nema, P. K. (2004). "Development of particle board from soybean husk without resin," *Journal of the Institutions of Engineers (India): Agricultural Engineering Division* 85, 5-9.

Sasaki, H. (1980). "Effective utilization of forest resources and research development of wood-based materials," *Wood Ind.* 35, 550-559.

Sihtola, H., and Neimo, L. (1975). "The structure and properties of cellulose," In: *Symp. on Enz. Hyd. of Cellulose*, Bailey, M., Enari, T.M., and Linko, M. (eds.), p. 9. SITRA, Helsinki.

Suzuki, S., Shintani, H., Park, S. Y., Saito, K., Laemsak, N., Okuma, M., and Iiyama, K. (1998). "Preparation of binderless boards from steam exploded pulps of oil palm (*Elaeis guineensis* Jaxq.) fronds and structural characteristics of lignin and wall polysaccharides in steam exploded pulps to be discussed for self-bindings," *Holzforschung.* 52, 417-426.)

Velásquez, J. A., Ferrando, F., Farriol, X., and Salvadó, J. (2003). "Binderless fiberboard from steam exploded *Miscanthus sinensis*," *Wood Sci. Technol.* 37, 269-278.

Xu, J., Han, G., Wong, E. D., and Kawai, S. (2003). "Development of binderless particleboard from kenaf core using steam-injection pressing," *J. Wood Sci.* 49, 327-332.

Article submitted: November 29, 2012; Peer review completed: January 4, 2013; Revised version received and accepted: February 5, 2013; Published: February 11, 2013.

Erratum changes made July 23, 2014: Some details, not affecting the conclusions, were corrected or clarified. Numerical values in columns 3, 4, 6, and 7 of Table 1 were corrected to match the experimental design points, to be more precise about what was done. Above Fig. 4, the value "12%" was changed to "12.91%". A redundant sentence was removed on page 1686 to avoid confusion. On page 1690, the following clarifying statement was added: "The rise of steaming time and steaming temperature decreases the water absorption property of the board." The following words were added to Conclusion 4: "From actual experiments".